JOURNAL OF MATERIALS SCIENCE 29 (1994) 978–986

The extent of microcracking and the morphology of microcracks in damaged bone

P. ZIOUPOS, J. D. CURREY
Department of Biology, University of York, York Y01 5DD, UK

Strain-induced damage in bovine laminar bone has been examined using laser scanning confocal microscopy (LSCM). The specimens were loaded in a fluorescein solution, which penetrated the newly formed cracks in the specimen. The microcracking, and the larger cracking, induced by strain were very clearly visible. The microcracking occurred diffusely in regions of high strain (stress), but was particularly obvious in the vicinity of large machined stress-concentrators. The microcracking could be shown not to be artefactual, that is, it was produced by strain, and not by specimen preparation. The microcracking interacted with the structure of the bone, often having a wavy appearance related to the histology. Microcracks seemed to be particularly associated with the most highly mineralized parts of the bone. LSCM is a technique holding great promise for the investigation of the initiation and development of damage in mineralized hard tissues, and other translucent materials.

1. Introduction

In recent years it has become increasingly apparent that a fruitful way of considering the mechanical behaviour of bone, after yield but before a fatal crack starts to spread through it, is to regard it as being affected by some kind of damage occurring in the material [1–5]. "Damage" is the term used in engineering for the result of any process that impairs the mechanical properties of a material [6–9].

Damage is shown particularly by the increased compliance of a material, after cyclic loading (as shown, for instance, in bone [10]) and it is in this sense that the term "damage" will be used in this paper. The increase in compliance, as seen by a drop in the secant modulus occurring in the post-yield region in single monotonic loading, is not necessarily caused by damage. For instance, in metals, post-yield behaviour can often be attributed to the movement of dislocations; in polymers, crazing, producing locally very high strains, and a concomitant local decrease in density of the material, has some similar phenomenological effects. In composites, microcracking often occurs, either within the stiffer phase, or at the interface between the stiffer and more compliant phase. A clear difference between ductile metals and the other materials is that movement of dislocations, and the plastic behaviour it produces, does not lead to a change in elastic modulus if the metal is unloaded and then reloaded. Therefore, in the case of plastics and composites the increased compliance indicates damage, in the case of the ductile metals it does not. For damage to occur in materials such as plastics and composites the stress or strain has often to exceed some threshold value. This is also the case in bone [11]. The increased compliance after the threshold is reached has been attributed to damage [3, 4]. The question is: what is the nature of this putative damage in bone?

An obvious answer is that damage is the formation of small cracks in the bony material which, for some reason, do not join to form large fatal cracks. Dispersed microcracking would result in an alteration of the bone's properties, by producing an increase in compliance, in a continuous and uniform fashion. However, it is strange that the reports in the literature of microcracking in bone are scarce, and any small cracks reported seem to be rather scanty and often very ill-characterized.

Martin and Burr [12] give a good review of the literature on cracks in bone, albeit with a strong emphasis on fatigue, and Frost has continually emphasized the importance of small cracks in fatigue [13]. Netz *et al.* [14] discuss cracking appearing in bone loaded in torsion. The features resulting from high compressive stresses show the characteristic appearance of shear cracks: they are rather straight, and they radiate at regular angles from small stress concentrators like blood channels [11, 15, 16]. These lines are usually attributed, probably correctly, to microbuckling of the lamellae in the bone.

In life, however, bones usually do not fail in compression, but in tension or shear. Cracks in regions exposed to tensile stresses are much more difficult to make out. Indeed, Tschantz and Rutishauser [16] write (p. 238): "In cortical bone in tension there are no oblique lines; the first visible damage is the fracture itself" (our translation).

However, Currey and Brear [17] were able to visualize, routinely but vaguely, features that they thought were cracks. These cracks did not seem to have their origin at small stress concentrators such as

0022–2461

blood channels, and they were much more diffuse than the features seen in bone loaded in compression.

Other evidence that microcracking occurs in bone and that it is associated with mechanical events comes from the optical effects associated with tensile yield: previously translucent bone becomes opaque and highly scattering when loaded into the yield region [11] and this opacity spreads from large stress concentrations such as notches, if such exist [18], but otherwise arises generally in the body of the specimen.

The load–deformation curve of bone loaded in tension has a relatively long post-yield region [19]. (We emphasize that by using the word "yield" we are making no assumptions about the mechanism that produces the characteristically sharp change in the slope of the load–deformation curve.) In an unnotched bone specimen, yield may occur at a strain of 0.005, whereas the ultimate strain may be 0.02. In antler, which can be considered, for materials science purposes, just to be poorly mineralized bone, the ultimate strain may be 0.10 [20]. In bones of various mineralization levels, it has been found that apparently irreversible damage starts at the same strain value of about 0.005 [21] while the ability of a bone specimen to stay in one piece (and thus still perform its duties moderately) is a function of it being able to undergo an extended post-yield deformation. If this considerable post-yield strain is caused by the opening up of little cracks, it is clear that they must be pervasive. It is somewhat of an embarrassment, therefore, that the evidence for microcracking is so vague.

Because microcracking is, to a large extent, concealed inside compact bone specimens, some invasive (preferably non-destructive) viewing method is needed in order to visualize the cracks *in situ*. Early results [17] using stains such as methylene blue showed a diffuse staining of loaded bone tissue, but this image could not be quantified and the third dimension could not be visualized. The use of conventional microtome sectioning is impractical and viewing by X-rays does not offer adequate resolution.

However, confocal microscopy can perform optical sectioning of a three-dimensional translucent object and is a promising option. In recent years the use of laser illuminating sources and digital acquisition and data processing equipment has greatly improved the potential of scanning confocal microscopy. Laser illumination offers the advantages of monochromatic light, small divergence, high brightness and a high degree of spatial resolution.

By the use of laser light tuned to the particular excitation level of fluorophore dyes, one can achieve excellent contrast between the site of the dye molecules and the background intensity levels, and the signal-to-noise ratio is very high. However, the contrast is also a function of absorption, fluorescence, reflections, refractions, scattering and so on, so the result can vary from application to application. Additional problems can be introduced by self-shadowing of an object, whereby more superficial fluorescing parts of an object blur the image of deeper lying segments [22]. Illumination in the presence of oxygen may produce photodamage, which can be reduced by protective chemicals [23]. However, the scanning mode of illumination, in which the laser sweeps past each spot, provides intense bursts of energy input instead of a continuous damaging illumination, thus making the most use of the dye.

The purpose of this work was to demonstrate, using laser scanning confocal microscopy (LSCM), that bone undergoes considerable microcracking, and that these cracks are of a size and shape as to be likely to lead to the effects seen at the phenomenological level.

2. Materials and methods

2.1. Scanning confocal microscopy

Images of microcracking in bovine bone were obtained by the use of a BIO-RAD MRC 600 Series LSC system and work station, using a krypton/argon mixed-gas laser which emits strongly at 488, 568 and 647 nm. The LSC system was attached to a NIKON Diaphot Inverted Fluorescence microscope. The data were stored on optical disks and were visualized, analyzed, and processed by the use of "Thru-View" software. A Sony UP 5000P video printer was attached to provide prints of black/white and pseudocoloured images.

The main advantage of the confocal microscope is that it can focus on a small spot at a defined level inside the specimen. The scanning mode produces a thin inner optical section of the specimen, which can be stored as a two-dimensional x–y image. Successive focussing at different depths adds a third z-dimension to the image. The three-dimensional image then consists of the so-called voxels, analogous to the well-known two-dimensional pixels.

The software allows various options. Thin-image sections in the z-dimension can be added together to a give, in "projection", a two-dimensional picture, which conveys more information than a conventional light-microscope image because it is in focus throughout the whole depth of the specimen. The three-dimensional voxel information can be "rotated", "displayed side by side" and "pseudo-coloured" according to depth or intensity. Digital filtering can also "crisp" images by clearing some of the noise.

2.2. Specimen preparation and loading

Coupon-shaped laminar [24] bone specimens were prepared from tibias of cattle aged about 18 months old. The samples were originally 5–7 mm wide, 1.5 mm thick and 55–60 mm long, cut in a longitudinal direction with respect to the long axis of the bone, and in the radial plane. In this configuration the laminae could be easily made out from the side, running up and down the specimen/bone axis. In some of the specimens, circular holes were drilled or edge notches cut, in order to study the effects of the stress concentration they induce. An EXAKT diamond saw was used to cut the notches; this cut slowly and finely under constant water irrigation, causing minimal adventitious damage to the specimen. It produced a slot slightly wider than 0.3 mm, with a semicircular end.

TABLE I The details of the treatment given to the various specimens.

Number	Description	Size[a] (mm)	Cycle[b]	Maximum nominal stress or imposed load per cycle (MPa or (N))	Relax[c] (s)	Rate[d] (s^{-1})	Damage[e] (%)
CB10	Central	30	1	125	–	0.0011	
	650 μm hole	5.4	2	116	–	0.0011	
		1.3	3	113	–	0.0011	
			4	111	–	0.0011	
			5	106	–	0.0011	2
CB7	Central	30	1	110	–	0.0011	
	750 μm hole	5.4	2	100	–	0.0011	
		1.4	3	97	–	0.0011	
			4	86	–	0.0011	2
CB23	370 μm wide	36	1	90	–	0.0009	
	660 μm long	6.6	2	101	–	0.0009	5
	notch	1.4					
CB26	Pair of notches, 3	36	1	(100)	–	0.0009	
	mm and 1.5 mm	6.2	2	(100)	–	0.0009	
	either side, 6.7	1.4	3	(100)	–	0.0002	
	mm apart		4	(100)	–	0.0002	
			5	(100)	–	0.0002	
			6	(100)	120	0.0002	
			7	(100)	–	0.0002	3–7
CB39	Central	36	1	72	–	0.0009	
	600 μm hole	6.4	2	110	–	0.0009	
		1.3	3	110	–	0.0009	
			4	115	–	0.0009	5
CB33	Pair of 3 mm and	36	1	(100)	–	0.0009	
	1.5 mm notches	5.6	2	(100)	–	0.0009	
	on either side and	1.3	3	(100)	–	0.0002	
	an extra 3 mm		4	(100)	–	0.0002	
	notch in between.		5	(100)	120	0.0002	
	Distance between		6	(100)	–	0.0002	4–5
	adjacent notches						
	3 mm						

[a]All specimens were coupon-shaped, the three numbers are the gauge length, the breadth and the depth. [b] The treatment on each cycle. [c] The number of seconds at which the specimen was held at a particular extension at the end of the loading part of the cycle. [d]The nominal strain rate (extension given by crosshead travel divided by the gauge length, divided by time.
[e]Estimate of the final amount of damage inflicted on the specimen. We define damage as the percentage reduction of the specimen's stiffness in tension at the end of the cyclic regime.

The bone samples were polished to their final dimensions with progressively finer grades of carborundum paper and were finally brought to a mirror finish by the use of alumina powder. During the whole preparation the samples were kept under water.

The mechanical stresses and deformations in the specimens were produced using an Instron 1122 universal testing machine equipped with a set of grips inside a dye-solution container. Nominal strain rates in the range of $(2 \times 10^{-4}$–$10^{-3})\,s^{-1}$ were used.

Fluorescein, a fluorophore dye, which absorbs at approximately 490 nm and emits at 520 nm, was used [23]. A saturated solution in 70% methanol was made at room temperature using a magnetic stirrer for a couple of hours. This procedure resulted in a deep-red opaque solution which, when filtered, produced a crystal-clear yellow fluorescein solution. The test solution was stored in the dark. In the mechanical tests the test chamber was completely filled with fluorescein solution; the specimen and grips were fully immersed.

Table I gives the specimen number, cross-sectional area, gauge length, any introduced stress concentrators, load levels at different cycles, how long stress relaxation was allowed, rate of loading, and the estimate of the damage inflicted on the specimen. All specimens were loaded in tension.

The depth through which the cracks could be imaged was limited to a maximum of 0.3 mm. There were two causes of this depth limitation. The first was that the fluorescent dye has to diffuse inwards from the surface. A balance had to be struck between allowing insufficient time for the dye to penetrate the cracks, and allowing a longer time so that the dye could penetrate ever more deeply into the cracks, but could also diffuse more generally into the bony tissue, so obscuring the picture to some extent. The second limitation was that the bone tissue attenuated the laser beam rather rapidly.

3. Results

The figures we discuss here are chosen to illustrate particular features of the distribution and shape of the cracks. However, no other images we obtained contradict statements we make below.

3.1. General appearance

Fig. 1 shows the typical appearance of the specimens away from stress concentrators. This specimen (CB10) has been loaded to a general stress of about 110 MPa, which is near the yield stress for bone. The

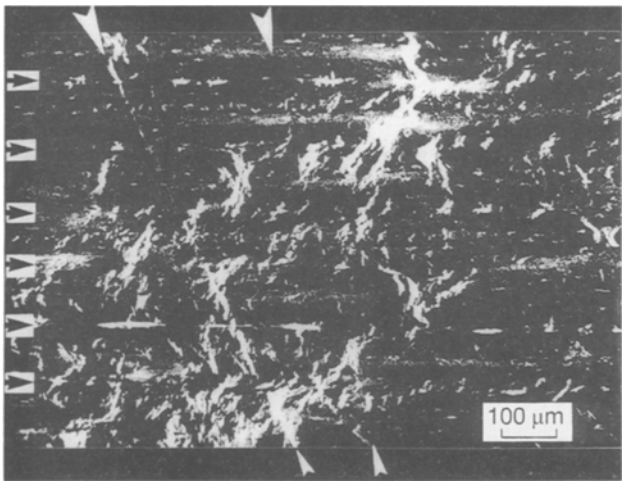

Figure 1 LSCM image of laminar bone (CB10) away from a region of high stress concentration. The direction of the tensile loading was horizontal. The diagonal lines (white arrows) are artefacts, stain has settled on surface scratches. The blood vessel networks, roughly 120 μm apart, are indicated by the black arrows. There are areas of diffuse cracking over all the image, and lines of intense but small cracks roughly midway between the lines of blood vessels. These are cracks originating in the most highly mineralized parts of the laminae.

load–deformation curve showed some slight yielding, probably mainly caused by localized yielding near a circular hole drilled through the middle of the specimen. The diagonal lines across the left and centre of the picture (white arrows) are artefacts caused by surface scratches; the dye has settled preferentially on them. The rest of the specimen shows bright areas, of two types of origin. There are bright areas associated with blood channels. These occur in lines (indicated by black arrows) and they are not cracks. The other bright areas are cracks. In this paper, by "cracks" we mean features of sharply delimited staining, not produced by blood channels, and not the extremely diffuse staining shown where the dye has penetrated the rather open structure of the woven bone (see below). Except for the largest ones, in which the two surfaces are separately visible, we have no direct evidence that these features are cracks. We cannot image the two surfaces, and it is possible that there may be some kind of microstructures present in the void. However, we presume that there must be some void because of the ease with which the stain reaches and stains them.

The cracks have two characteristics: they are diffuse, occurring widely over the specimen, and most of them are very short, the size distribution starting at the lower limit of resolution of the LSCM system. Some bright areas seem, however, quite long and large but, because the photograph is of the summed projection of about 20 images about 2 μm apart in depth, this does not necessarily imply that the cracks themselves are this large. We return to this point later, as we shall to the fact that the small cracks seem, in places, to be arranged in rows, parallel to the lines of blood channels.

Fig. 2 is typical of the general appearance of specimens in the vicinity of stress concentrators. The specimen (CB23) is mainly dark, but the vascular cavities are picked out as parallel stripes. The laminar structure of the specimen is evident. As in the picture described above, some highlights come from the stain that has diffused into the blood channels, and are not cracks. A slot has been cut into the specimen, which produces a stress concentration at its end. In just the place where the stress concentration will be greatest there are bright lines, looking like flames, emerging from the end of the slot. These "flames" are caused by the dye which has penetrated the cracks originating at the end of the slot. Note that there is none emerging from the sides of the slot, where stress is low.

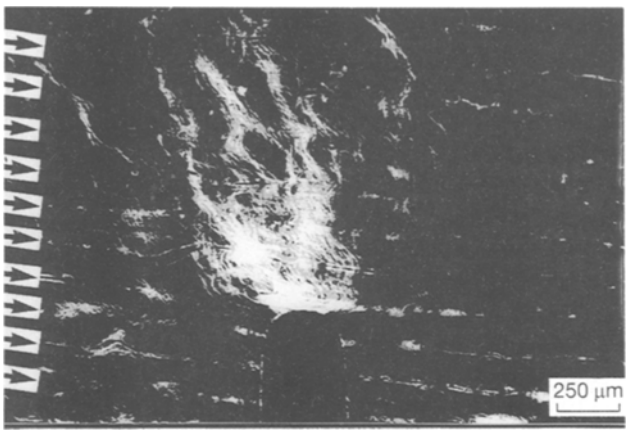

Figure 2 LSCM image of the distribution of cracks at the end of a stress concentrator (CB23). The rows of blood channels are indicated by black arrows.

3.2. Are the cracks artefacts produced by machining?

Fig. 3 shows a specimen (CB26) in which two slots have been machined. One slot (A) has a depth of 3 mm, the other (B) a depth of 1.5 mm. They are roughly 350–360 μm wide. The longer slot protected the shorter one from stress. There is some diffuse staining all over the specimen, and particularly in blood channels. (The white arrow points to a scratch.) However, there is very intense staining at the tip of the deep slot, but none at all at the tip of the shorter, stress-protected one. It is clear, therefore, that the act of machining slots does not produce stresses sufficient to cause microcracking.

3.3. What is the shape of the cracks in the third dimension?

Pictures taken from the side, as in Figs 2 and 3, show the projections of many images taken at successively greater depths. However, the LSCM can take optical slices, which can be shown on separate images. Fig. 4 shows five successive images (a–e) of some cracks, taken 5 μm apart. The apparent thickness of the cavity of the cracks varies from about 2–5 μm, and at any level they are about 10–50 μm long. Some of the cracks (e.g. arrowed "1") persist through all five sections, and so are at least 20 μm wide in the plane of the crack. Others (e.g. arrowed "2") do not appear in the more superficial image, but start deeper. Others (e.g. arrowed "3") are apparent in the superficial section, but later disappear.

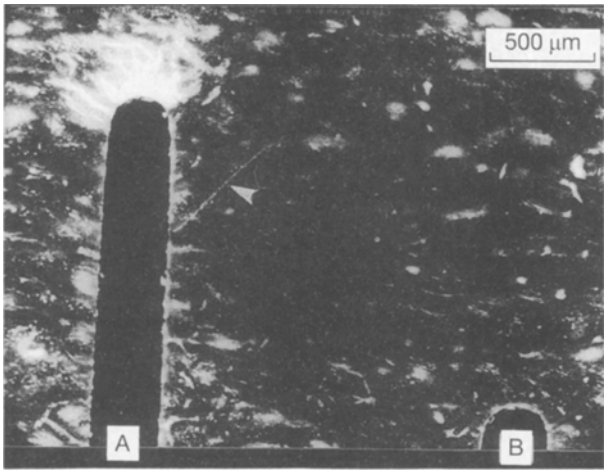

Figure 3 LSCM image showing the stress-shielding effect of a longer slot on a shorter one (CB26).

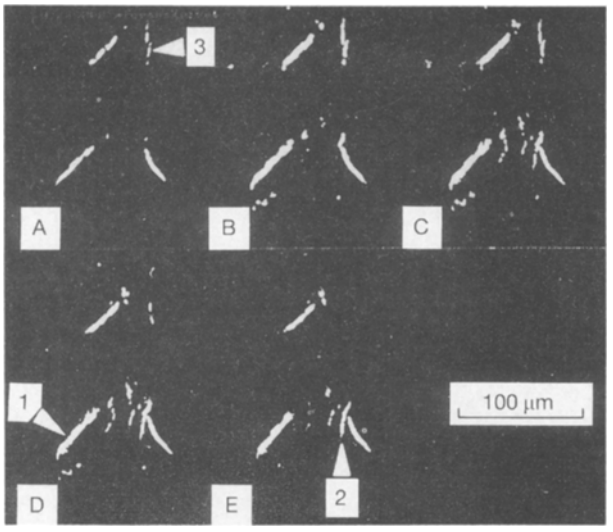

Figure 4 Five LSCM of some cracks taken at ever-increasing depths in the specimen (CB7); the images are 5 μm apart. Some cracks, e.g. "1" (arrowed), persist in all images; some, e.g. "2" (arrowed) appear only in the deeper images; some, e.g., "3" (arrowed) appear only in the more superficial images.

It is possible to obtain images of cracks in successive sections, merge the two images, and from this calculate the angle at which they are oriented in relation to the laser beam (and also to the long axis of the bone). In Fig. 5a one crack (arrowed "1") is oriented almost exactly in the plane of the laser beam; another, shown enlarged in Fig. 5b (arrowed "2"). is oriented at an angle of about 35° to the beam, being further to the top left of the image in the deeper section.

Because the information about every voxel (three-dimensional pixel) is held in the computer, it is possible to rotate the image of the cracks, as is shown in Fig. 6. Each image is of all the constituent images superimposed; the top left image is as viewed in the direction of the laser beam, the bottom right image is at 70° to this first image. The intervening pictures are each rotated through 10° relative to their neighbours. The cracks, which appear as relatively thin lines when viewed from the direction of the laser, are seen actually to be quite deep, at least 20 μm in this case. This is a

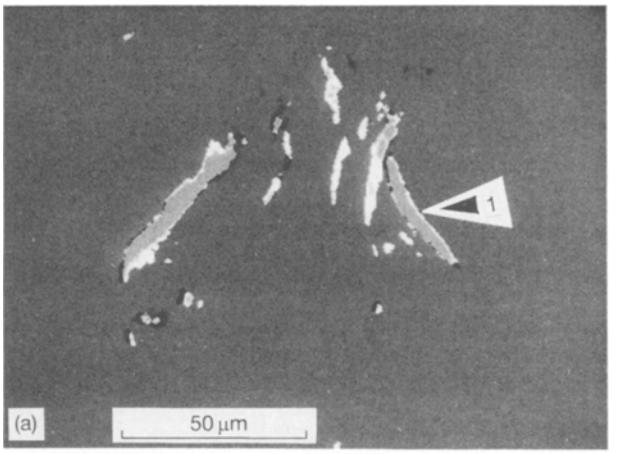

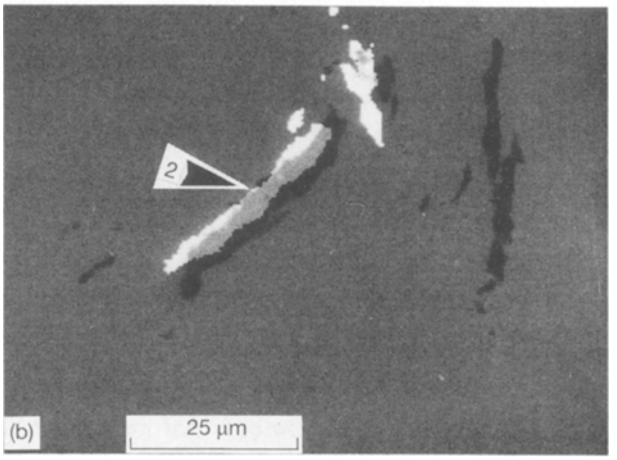

Figure 5(a) Two LSCM images differing in depth by 15 μm. (These are some of the cracks shown in Fig. 4.) One crack ("1" arrowed) has the images at the two depths (white and black) almost superimposed (grey). (b) as (a), at a larger scale. A crack ("2" arrowed) is oriented at about 35° to the laser beam. (The two images are much clearer on the original image, being false-coloured, with the region of overlap shown by a third colour.)

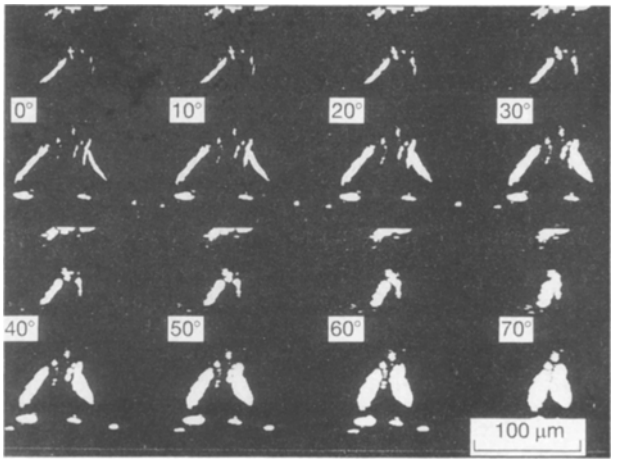

Figure 6 LSCM image (CB7), as shown in layers in Fig. 4. The images are now superimposed, and rotated in successive frames by 10°. The cracks, which in the first image are seen more or less thin-side on, are rotated until depth is revealed in the last few images.

minimum depth because, as explained previously, the penetration of the dye and the laser beam limit the depth of the image.

It is not possible to be precise about the thickness of the cracks. The dye presumably settles mainly on the

walls. However, it will also penetrate into the bone somewhat, thereby increasing the apparent thickness of the cracks. On the other hand, if the dye has difficulty in penetrating a crack, it may produce an apparent thickness less than the actual thickness.

3.4. What is relationship of the cracks to machined inhomogeneities in the specimen and to its histology?

We have already shown how the cracks develop from the end of slots. Fig.7 is another example. Holes in a specimen (CB39) loaded in tension would tend to develop high stresses at the equator normal to the direction of loading, and not at the poles in line with the direction of loading. The pattern of cracks is what is expected.

So far we have shown that the cracks visualized in the LSCM are in the appropriate places and are oriented roughly in the directions expected from the state of the local stress field. However, bone is not a uniform solid, it is anisotropic, and contains a number of inhomogeneities, which will themselves affect the stress field, and also make crack opening easier in some directions than in others. We now examine these interactions.

Fig. 8 is a diagram of the histological structure of laminar bone, which is the type of bone which has been tested here. Two-dimensional networks of blood vessels, lying about 120 μm apart, are sandwiched between layers of lamellar bone. Between adjacent layers of lamellar bone is a layer of woven-fibred bone [25, 26]. The woven-fibred bone is more highly mineralized than the lamellar bone [27]; it is also harder [28], and therefore probably has a higher Young's modulus than the lamellar bone [29]. Right in the middle of the sandwich is a narrow hypermineralized sheet, the "bright line" [30] where there is rather little collagen. (This sheet is called a cement line by Lakes and Saha [31] in their discussion of cement line motion. However it has a different origin from a cement line round a Haversian system, because cement lines (sheaths) are reversal lines, indicating the limit of erosion by osteoclasts, before new bone is laid on the surface. The bright line is not a reversal line, but is a line at which growth ceased for a while. Furthermore, it almost certainly is a line (sheet) of hypermineralization, whereas the cement line (sheath) is probably a line of hypomineralization [24, 32].)

The arrangement of the collagen fibrils and their associated mineral differs in the different layers. In the layers of lamellar bone, near the blood channels, the collagen is highly oriented in the plane of the lamellae, although its orientation *within* this layer is rather variable, that is, it may be oriented in the long axis of the bone in one lamellae, and then be nearly at right angles in the neighbouring lamellae. In the woven-fibred bone towards the middle of the sandwich the orientation of the collagen is much more varied, bearing no particular relationship to the plane of the layer. The orientation of collagen in the bright line is unknown, but there is rather little of it present.

Fig. 9 shows the results of cutting two slots in the specimen (CB33) from opposite sides. The stresses are high at the tips of the slots, and there are cracks there. However, this arrangements of slots also produces shear stresses along the line joining the slot tips. Fig. 10 is a "crisped", projected magnification of the region marked by an arrow in Fig. 9. It shows a row of little cracks oriented at about 30° to the long axis of the specimen. The direction of the cracks is as expected: the relative movements of the bone segments above and below the cracks, towards the right and left, respectively, cause the cracks to open up. Bone in unstressed parts of Fig. 9 (lettered arrows) shows a characteristic pattern of staining by the dye. The blood channels are picked out like rows of fairy lights. The bone immediately around them is dark. This is the

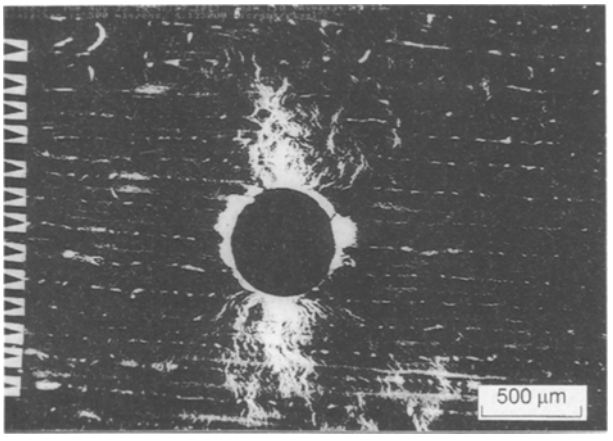

Figure 7 LSCM image of the distribution of cracks round a machined hole (CB39). The loading direction is horizontal. Layers of blood channels are indicated by arrows. The general ring of brightness round the hole is caused by a slight eccentricity of the drill producing a great deal of local damage. Compare this with Fig. 3, where the slot was produced by a precision saw, and very little staining is seen on the sides of the slot. Note how the dye settles in the blood channels and also in the highly mineralized region midway between layers of blood channels.

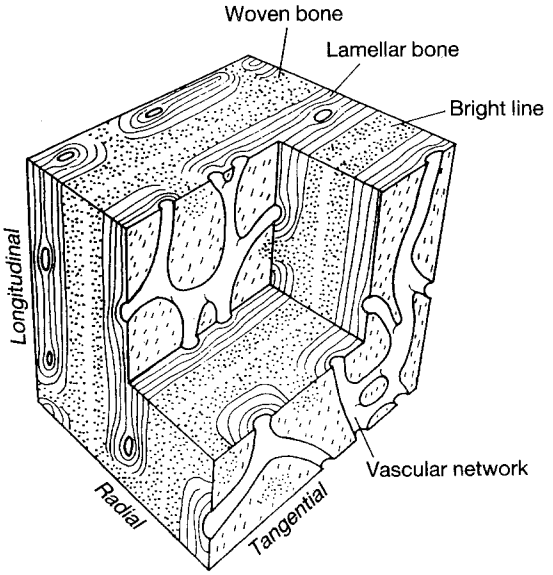

Figure 8 Block diagram of laminar bone showing the relative positions of the various features mentioned in the text. The distance between the vascular networks is from 100–200 μm in bones from different species.

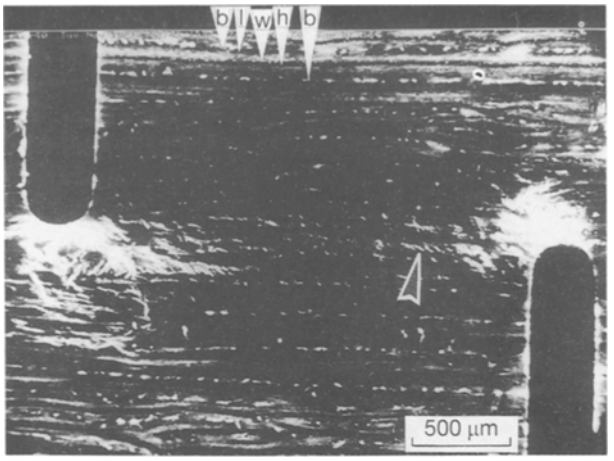

Figure 9 LSCM image of cracks emanating from two slots cut on opposites sides of a test specimen (CB33). The labelled arrows point to various histological features: b, blood channel; h, hypermineralized sheet; l, lamellar bone; w, woven bone. The region indicated by the unlabelled arrow is shown magnified in Fig. 10.

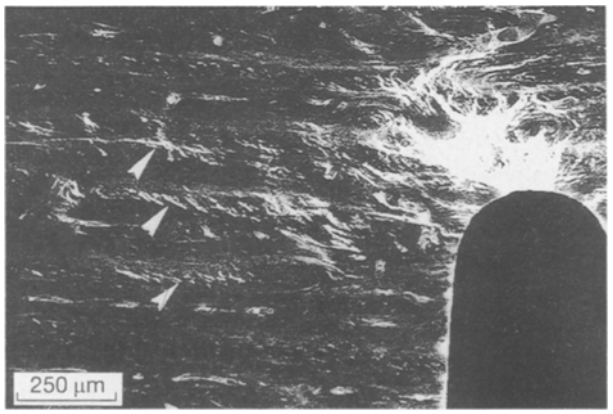

Figure 10 Enlarged view of part of Fig. 9 (CB33), showing the little cracks (arrowed) mainly restricted to the heavily mineralized region.

lamellar bone, which is dense, and into which the dye has difficulty in penetrating. Further from the blood channels the dye penetrates to some extent forming a continuous hazy line, where the dye penetrates the looser-textured woven-fibred, though more highly mineralized, bone. This line is interrupted, right at the middle, by a dark region. This is the position of the highly mineralized sheet. This pattern is seen clearly at the top of the figure, but is not seen so clearly elsewhere, and indeed the relative thicknesses of the various components of the sandwich vary from place to place according to the rate at which the bone was being laid down (the lower the rate of deposition the greater the thickness of each lamina that is taken up by lamellar rather than by woven bone).

Fig. 2 shows the pattern of cracks at the tip of a slot in laminar bone. The positions of the two-dimensional sheets of blood channels are indicated by arrows. The overall direction of the "flames" is inclined to the left, instead of going straight across the specimen. This is most probably an effect of the orientation of the laminae relative to the direction of load. The laminae are inclined somewhat from top left to bottom right. Laminar bone has considerable anisotropy in strength [33], the strength in the direction of the long axes of the laminae being about three times that in the radial direction. This anisotropy will, of course, tend to cause cracks to align themselves more in the direction of the laminae, if these are inclined to the direction of the principal stress. The extent to which this happens will depend on the amount of the anisotropy. Behiri and Bonfield [34] showed that in compact tension specimens the crack tended to travel longitudinally along the bone specimen, and so they had to groove the specimens to force the cracks to travel in the desired direction.

The cracks are wavy, and the period of the waves is the same as that of the laminar sheets. Those cracks that run overall roughly normal to the sheets generally pass the layer of blood vessels in a direction normal to the sheet, then swing off at an angle before returning to a normal direction for the next sheet. In many places the microcracking is less in the actual line (plane) of the blood vessels and denser and thicker in the part of the lamina roughly furthest from the blood channels (arrows). Probably the lamellar bone round the blood vessels is stronger than the woven bone, and the transverse orientation of the blood channels acts as a moderate barrier to the spread of the microcracks between laminae. The microcracks tend to coalesce midway between the vascular networks producing what we might call a mesocrack, say 100 μm long. There are many cracks not connected at all with the main body of the flames in the vicinity of the notch. This shows that the cracking is not simply the spread of a single crack, but is the general reaction of the tissue to locally high stresses. The cracks initiate, but do not spread.

It is also clear that the cracks interact with the structure of the bone. The grain of the bone does not allow the cracks to travel in straight lines. The layers of the laminae are geometric/anatomical features, similar to each other in their composition, unlike composites where stiff/strong laminae are loosely adherent to each other. However, their presence seems to have influenced the coalescence of the microcracks.

Fig. 10, of the sheared region between two notches, shows that the short shear cracks have their origin near, and probably at, the hypermineralized sheet (arrows). The short cracks extend to varying extents in the woven-fibred bone on each side, but, in these specimens at least, do not extend far if at all, into the less mineralized and more highly organized lamellar bone bordering the blood channels.

4. Discussion

A prerequisite for the full understanding of bone mechanics and the modelling of bone's mechanical behavior is that the mechanisms that govern the deformation and failure of the tissue in the post-yield region are clarified. The real state of affairs as to the existence and spread of microcracks has proved to be very elusive. The use of the LSCM has allowed, for the first time, the visualization of small cracks with such a clarity that the qualitative outcome of their presence is immediately evident and also makes quantification in the future a real possibility.

For this preliminary study, bovine laminar bone, which is highly ordered, was loaded in tension. Microcracking appeared in places where it would be expected to exist in relation to mechanically induced stress concentrations, such as slots and holes. The microcracks have, in many places, the wavy appearance noted by Currey and Brear [17]. They do not originate from small stress concentrators such as vascular channels. However, in the regions of high stress and strain they appear in a diffuse manner, probably beneficial for the integrity of the tissue. Pervasive cracks tens of micrometres long and wide exist only a few micrometres away from each other without coalescing.

Earlier workers, assuming (or hoping) that bone could be modelled as a linear elastic material, have suggested that it would be easier, and therefore more important, to prevent, the appearance of the first crack than to arrest its catastrophic course [35, 36]. However, the great number of small microcracks demonstrated in the present study, and their apparent insensitivity to each other's existence, suggest that what really matters is not to prevent the appearance of microcracks, but to stop them from growing and communicating with each other. This finding is in agreement with the suggestions of later workers in the field [12, 37].

A consequence of the presence and extent of microcracking in bone is that it may justify the use of continuum damage mechanics (CDM) theories to model bone's mechanical behaviour. The mechanical importance of newly formed microsurfaces opening up inside a compact body is that the integrity of the tissue is impaired, and the modulus of elasticity is reduced. CDM has been formulated to provide a macroscopic description of the materials's properties viewed as a continuum in the presence of microcracks. Krajcinovic *et al.* [4] derived a simple constitutive model for cortical bone using the damage approach without any real evidence of the morphology of microcracking. They considered Haversian bone only, and assumed that, until the fatal crack developed, *all* the microcracking in the bone took place at the cement lines surrounding Haversian systems. They assumed that the cement lines (which are, of course, actually sheaths) were hypermineralized and brittle. In fact, it is probable that they are hypomineralized and viscous [12, 32]. However, for the damage approach as taken by Krajcinovic *et al.* [4], the difference may not be very important, as long as the cement line is weaker than the other parts of the bone. Clearly, the shape, size and nature of microcracking in Haversian bone needs to be looked at with the LSCM technique.

Our results also shed some light on the question of the sites of weakness in the bone's structure. Well-mineralized bone appears macroscopically to fail in a brittle fashion. Many years ago, Currey [26] suggested that voids, vascular spaces and other pores, which normally exist in bone, might act as stress concentrators and that the final fatal crack could be initiated from one of them. In the years that followed, the majority of bone biomechanics thoughts concerning fracture developed along these lines, leading to the application of linear elastic fracture mechanics (LEFM) to fracture in bone. The idea of an *intrinsic crack length* was introduced [38] and values (for an edge crack) between 340 μm [39], 360 μm [37], 1.8 mm [40] or even greater [38] were calculated for it. Consequently, researchers tried to identify those features (voids, pores and so on) in the structure of bone that would agree with dimensions of these sizes, without much success [39].

In the present study we found no evidence to suggest that vascular or other naturally occurring cavities initiated cracking in laminar bone loaded in tension. The hollow vascular spaces in laminar bone appeared adequately "armoured" (reinforced), cracks did not originate from them, and indeed they were usually able to deflect the microcracking, which circumvented them. Microcracking of the bone tissue was clearly related to the stress or strain experienced by the tissue locally. If one still wishes to assign some physical meaning to the values of the "intrinsic crack length" for cortical bone, one should relate it to the amount and local density of microcracking in the tissue that actually exist, rather than to the dimensions of holes in the tissue that do not exist.

Finally, the examination of microcracking in highly ordered laminar bone showed that it was, in general: (i) dispersed, (ii) structure-related, with the local heterogeneity of the tissue being able to incline and as a whole direct the cracks towards one of the tissue's axes of anisotropy, (iii) preferentially oriented, with the newly opened surfaces being normal to the tensile field, (iv) definitely associated with the more highly mineralized parts of the tissue.

Acknowledgements

We are grateful to the American Air Force Office of Scientific Research for supporting us with a grant to investigate toughening mechanisms in biological hard tissues, and the Science and Engineering Research Council for making available the Scanning Confocal Microscope. We thank Professor John Tucker, Dr Mette Mogensen, and John Mackie, at St Andrews for letting us use the Scottish Confocal Microscope Facility, and for helping in its operation.

References

1. W. E. CALER and D. R. CARTER *J. Biomech.* **22** (1989) 625.
2. D. R. CARTER and W. E. CALER, *J. Orth. Res.* **3** (1985) 84.
3. J. D. CURREY, *J. Biomech.* **22** (1989) 469.
4. D. KRAJCINOVIC, J. TRAFIMOW and D. SUMARAC, *ibid.* **20** (1987) 779.
5. P. ZIOUPOS, A. J. SEDMAN and J. D. CURREY, in "VIII Meeting of the European Society of Biomechanics", Edited by P. Belloti and A. Cappozzo Rome (1992) p. 41.
6. C. L. CHOW and T. J. LIU, *int. J. Fract.* **50** (1991) 79.
7. D. KRAJCINOVIC, *Appl. Mech. Rev.* **37** (1984) 1.
8. P. LADEVEZE, in "Mechanics and Mechanisms of damage in composites and multi-materials", ESIS11, edited by D. Baptiste (Mechanical Engineering Publications, London, 1991) p. 119.
9. M. H. J. W. PAAS, P. J. G. SCHREURS, C. W. J. OOMENS and J. D. JANSSEN, *ibid.*, p. 159.

10. C. A. PATTIN, D. R. CARTER and W. E. CALER, in "Proceedings of the 36th ORS Meeting", New Orleans (1990) p. 90.
11. A. H. BURSTEIN, D. T. REILLY and V. H. FRANKEL, in "Perspectives in biomedical engineering", edited by R. M. Kenedi (Macmillan, London, 1973) p. 131.
12. R. B. MARTIN and D. N. BURR, "Structure, function, and adaptation of compact bone" (Raven Press, New York, 1989).
13. H. M. FROST, *Calc. Tiss. Int.* **44** (1989) 367.
14. P. NETZ, K. ERIKSSON and L. STROMBERG. *Acta Orthop. Scand.* **51** (1980) 223.
15. A. J. CHAMAY, *J. Biomech.* **3** (1970) 263.
16. P. TSCHANTZ and E. RUTISHAUSER, *Ann. Anat. Path.* **12** (1967) 223.
17. J. D. CURREY and K. BREAR, *Calc. Tiss. Res.* **15** (1974) 173.
18. A. J. SEDMAN, J. D. CURREY and P. ZIOUPOS, in "VIII Meeting of the European Society of Biomechanics", Rome (1992) p. 40.
19. D. T. REILLY and A. H. BURSTEIN, *J. Bone Joint Surg.* **56-A** (1974) 1001.
20. J. D. CURREY, *J. Biomech.* **23** (1990) 837.
21. J. D. CURREY, A. J. SEDMAN and P. ZIOUPOS, in "VIII Meeting of the European Society of Biomechanics", Rome (1992) p. 50.
22. P. C. CHENG and R. G. SUMMERS, in "Handbook of Biological Confocal Microscopy", edited by J. B. Pawley (Plenum, New York, 1990) p. 179.
23. R. T. TSIEN and A. WAGGONER, *ibid.*, p. 169.
24. H. FRANCILLON-VIEILLOT, V. DE BUFFRÉNIL, J. CASTANET, J. GÉRAUDIE, F. J. MEUNIER, J. Y. SIRE, L. ZYLBERBERG and A. de RICQLÈS, in "Skeletal Biomineralization: Patterns Processes and Evolutionary Trends", Vol. 1, edited by J. G. Carter (Van Nostrand Reinhold, New York, 1990) p. 471.
25. E. BROUWER, *Voeding* **13** (1952) 55.
26. J. D. CURREY, *Q. J. Microsc. Sci.* **101** (1960) 351.
27. A. ASCENZI, E. BONUCCI and D. S. BOCCIARELLI, *J. Ultrastruct. Res.* **18** (1967) 605.
28. P. KUCERA, *Folia Morph.* **13** (1965) 71.
29. J. D. CURREY and K. BREAR, *J. Mater. Sci. Mater. Med.* **1** (1990) 14.
30. J. D. CURREY, *Q. J. Microsc. Sci.* **103** (1962) 111.
31. R. LAKES and S. SAHA, *Science* **204** (1979) 501.
32. M. B. SCHAFFLER, D. B. BURR and R. G. FREDERICKSON, *Anat. Rec.* **217** (1987) 223.
33. D. T. REILLY and A. H. BURSTEIN, *J. Biomech.* **8** (1975) 393.
34. J. C. BEHIRI and W. BONFIELD, *ibid.*, **22** (1989) 863.
35. W. BONFIELD and P. K. DATTA, *J. Mater. Sci.* **8** (1974) 1590.
36. M. H. POPE and J. O. OUTWATER, *J. Biomech.* **5** (1972) 457.
37. D. MARGEL-ROBERTSON, D. ROBERTSON and C. R. BASSETT, *ibid.* **11** (1977) 359.
38. K. PIEKARSKI, *J. Appl. Phys.* **41** (1970) 215.
39. W. BONFIELD and P. K. DATTA, *J. Biomech.* **9** (1976) 131.
40. D. D. MOYLE and A. J. GAVENS, *ibid.* **19** (1986) 919.

Received 26 January
and accepted 24 August 1993